FEBS Letters

FEBS PRESS
science publishing by scientists

Cancer-associated mutations in human pyruvate kinase M2 impair enzyme activity

Vivian M. Liu[1,2], Andrea J. Howell[1], Aaron M. Hosios[1], Zhaoqi Li[1], William J. Israelsen[1,3] and Matthew G. Vander Heiden[1,4]

1 David H. Koch Institute for Integrative Cancer Research, Massachusetts Institute of Technology, Cambridge, MA, USA
2 Harvard-MIT Health Sciences and Technology Division, Harvard Medical School, Boston, MA, USA
3 Department of Biochemistry, University of Texas Southwestern Medical Center, Dallas, TX, USA
4 Dana-Farber Cancer Institute, Boston, MA, USA

Correspondence
W. J. Israelsen, Department of Biochemistry, University of Texas Southwestern Medical Center, Dallas, Texas, 75390, USA and M. G. Vander Heiden, David H. Koch Institute for Integrative Cancer Research, Massachusetts Institute of Technology, Cambridge, Massachusetts, 02139, USA
Tel: +1 214 648 3348 (WJI); +1 617 715 4471 (MGVH)
E-mails: william.israelsen@utsouthwestern.edu (WJI); mvh@mit.edu (MGVH)

Vivian M. Liu and Andrea J. Howell have equal contribution

(Received 8 July 2019, revised 28 September 2019, accepted 15 October 2019)

doi:10.1002/1873-3468.13648

Edited by Judit Ovádi

Mammalian pyruvate kinase catalyzes the final step of glycolysis, and its M2 isoform (PKM2) is widely expressed in proliferative tissues. Mutations in PKM2 are found in some human cancers; however, the effects of these mutations on enzyme activity and regulation are unknown. Here, we characterized five cancer-associated PKM2 mutations, occurring at various locations on the enzyme, with respect to substrate kinetics and activation by the allosteric activator fructose-1,6-bisphosphate (FBP). The mutants exhibit reduced maximal velocity, reduced substrate affinity, and/or altered activation by FBP. The kinetic parameters of five additional PKM2 mutants that have been used to study enzyme function or regulation also demonstrate the deleterious effects of mutations on PKM2 function. Our findings indicate that PKM2 is sensitive to many amino acid changes and support the hypothesis that decreased PKM2 activity is selected for in rapidly proliferating cells.

Keywords: allostery; cancer; enzymology; mutation

Mammalian pyruvate kinase isoforms function as homotetramers to catalyze the final step of glycolysis, which is the transfer of phosphate from phosphoenolpyruvate (PEP) to ADP to produce pyruvate and ATP. There are four mammalian pyruvate kinase isoforms, and the activity of each isoform is regulated in a manner that suits its physiological role [1–3]. The muscle (PKM1) isoform is found in nonproliferating and highly catabolic tissues such as the heart, brain, and skeletal muscle, where it functions as a highly active, constitutive tetramer with few regulatory inputs [1,2,4–7]. The liver (PKL) and red blood cell (PKR) isoforms are subject to allosteric feed-forward activation by an upstream glycolytic intermediate, fructose-1,6-bisphosphate (FBP) [8,9]. Both of these enzymes are also inhibited by phosphorylation, with the liver isoform regulated to minimize futile cycles during gluconeogenesis [10]. The M2 isoform of pyruvate kinase (PKM2) is expressed in most other

Abbreviations
BME, β-mercaptoethanol; CV, column volumes; FBP, fructose-1,6-bisphosphate; hPKM2, human PKM2; IPTG, isopropyl-D-1-thiogalactopyranoside; Ni-NTA, nickel-nitriloacetic acid; PEP, phosphoenolpyruvate; PKM2, M2 isoform of pyruvate kinase; TCGA, The Cancer Genome Atlas.

tissue types, including the developing embryo and virtually all cancers and proliferative tissues studied to date [1,2,4,11]. In proliferating tissues, PKM2 catalytic activity is tightly regulated to balance the catabolic and anabolic needs of proliferating cells [12,13].

PKM2 activity is modulated by a host of regulatory inputs. Like PKL and PKR, FBP is a major allosteric activator of PKM2 [14,15], and its activity is also affected by other allosteric effectors, including thyroid hormone T_3, serine, phenylalanine, and select other amino acids [7,16–19]. FBP binding increases affinity of PKM2 for one of its substrates, PEP, and stabilizes the PKM2 tetramer in a fully active conformation [15,20]. The PKM2 tetramer assembles as a dimer of dimers, and the enzyme exists in a tetramer-dimer-monomer equilibrium with the less-active, FBP-free, tetramer conformation prone to dissociation to inactive dimers and monomers. Tetramer dissociation significantly reduces enzyme activity, while the binding of FBP favors tetramer assembly and results in an increase in V_{max} due to an apparent increase in concentration of functional enzyme [7,16]. This association–dissociation phenomenon is also observed *in vivo* [20–22].

Release of FBP, and subsequent downregulation of enzyme activity, is stimulated by interaction of the enzyme FBP-binding pocket with tyrosine-phosphorylated proteins generated by growth signaling [23]. Additional mechanisms can also reduce pyruvate kinase activity in proliferating cells including lysine acetylation, cysteine oxidation, and degradation of the enzyme in nutrient-replete conditions [24,25]. Reduction of PKM2 activity *via* intracellular signaling may facilitate biosynthesis [26], and genetic or pharmacologic activation of pyruvate kinase disrupts proliferative metabolism and is detrimental to tumor growth [20,27,28]. Decreased pyruvate kinase activity seems particularly important for nucleobase synthesis [28], and genetic experiments using mouse cancer models suggest that loss of pyruvate kinase activity can be selected for in tumors [11,29].

We reported heterozygous mis-sense mutations in PKM2 that were found in human cancers [29]. Here, we consider mutations in PKM2 reported in The Cancer Genome Atlas (TCGA) affecting 23 amino acids throughout the tertiary structure of the enzyme (Fig. S1). Each PKM2 subunit contains three main domains: the A domain, a TIM barrel that hosts the active site; the B domain, which closes down on the active site during substrate binding and catalysis; and the C domain, which comprises most of the dimer-dimer interface and contains the FBP-binding site [30,31] (Fig. S1C). Pyruvate kinase is highly conserved, and PKM2 function appears to be sensitive to amino acid substitutions, even in solvent-exposed residues [32], suggesting that the PKM2 mutations occurring in human tumors may affect the enzyme activity. Given that a reduction in intracellular pyruvate kinase activity supports proliferative metabolism [2,20,24,28,29], we hypothesized that these cancer-associated mutations may reduce or abolish PKM2 pyruvate kinase activity.

Nonglycolytic signaling functions of PKM2 have also been proposed as an alternative explanation for PKM2 selection in cancer [12,33,34]. In this context, amino acid substitutions in PKM2 have been used to experimentally separate the proposed nonglycolytic functions from the role of the enzyme in glycolysis [35,36], or to alter the response of the enzyme to other allosteric inputs [17,23]. While some pyruvate kinase enzyme activity is retained in these mutants, the effects of these mutations on enzyme kinetics have not been well characterized. To understand how these mutations affect PKM2 function in proliferating cells, kinetic characterization is necessary, particularly in light of controversy surrounding the proposed functions of PKM2 [3,37].

Experimental procedures

PCR mutagenesis

PCR mutagenesis was used to generate mutations in the coding sequence of the human PKM2 (hPKM2) cDNA cloned into pET-28a with an in-frame N-terminal 6x-His tag [23]. The conditions for PCR mutagenesis were: 90 s at 98 °C, followed by 16 cycles of 10 s at 98 °C, 30 s at 55 °C, and 10 min at 72 °C, with an additional 10 min final elongation step at 72 °C. The forward primers used were as follows (5′-3′, underlined bases indicate mutations):

S37A: CGCCTGGACATTGATTACCCACCCATCACAGCC;

P117L: CTAGACACTAAAGGACTTGAGATCCGAACTGGG;

R246S: TTTGCGTCATTCATCAGCAAGGCATCTGATGTC;

K367M: TCTGGAGAAACAGCCATGGGGGACTATCCTCTG;

R399E: TTATTTGAGGAACTCGAACGCCTGGCGCCCATT;

G415R: GAAGCCACCGCCGTGCGTGCCGTGGAGGCCTCC;

K433E: ATAATCGTCCTCACCGAGTCTGGCAGGTCTGCT;

R455Q: ATCATTGCTGTGACCCAGAATCCCCAGACAGCT;

H464A: ACAGCTCGTCAGGCCGCCCTGTACCGTGGCATC;

R516C: GTGCTGACCGGATGGTGCCCTGGCTCCGGCTTC.

The reverse primer sequences are the reverse complement of the forward primers. Successful mutagenesis was verified by sequencing the coding region of the plasmid using T7 promoter and terminator primers.

Native protein expression

Wild-type and mutant PKM2 6x-His-tagged proteins were expressed in *Escherichia coli* BL21(DE3) and the soluble protein was purified from the cell lysates. A 50-mL starter culture was inoculated with a colony of freshly transformed *E. coli* and grown at 37 °C overnight in LB broth containing 50 $\mu g \cdot mL^{-1}$ of kanamycin (LB-kan). The starter culture was diluted 1/40 into 1 L of LB-kan containing 2 mM $MgCl_2$. The expression culture was grown at 37 °C till an OD_{600} of 0.7 was obtained and induced for 6 h at 25 °C with 0.5 mM isopropyl-D-1-thiogalactopyranoside (IPTG). Following centrifugation, the cell pellet was snap-frozen using liquid nitrogen and stored at −80 °C prior to subsequent purification.

Protein preparation 1: One-column PKM2 purification

Escherichia coli BL21(DE3) cells were transformed, induced, pelleted, and frozen as described in the section 'Native protein expression' above. All protein purification steps were performed on ice or at 4 °C. The cell pellet was resuspended in buffer C (50 mM Tris, pH 8.5; 10 mM $MgCl_2$; 300 mM NaCl; 10% glycerol; 5 mM imidazole), lysed by sonication, and clarified prior to supernatant collection and addition of β-mercaptoethanol (BME) to 0.1% (v/v) final concentration. Recombinant protein was batch-bound to nickel-nitriloacetic acid (Ni-NTA) agarose beads (Qiagen 30210, 4 mL bead volume per 1 L of culture; Germantown, MD, USA). Beads were batch-washed four times with 30 mL of buffer D (50 mM Tris, pH 8.5, 10 mM $MgCl_2$, 300 mM NaCl, 10% glycerol, 30 mM imidazole) and packed into a gravity flow column at 4 °C. Protein was eluted with buffer E (50 mM Tris, pH 8.5, 10 mM $MgCl_2$, 250 mM NaCl, 10% glycerol, 250 mM imidazole) and collected in 1-mL fractions. The three fractions containing the peak of eluted protein were identified using the Bradford assay, pooled, and dialyzed against 1 L of buffer F (50 mM Tris, pH 7.5, 10 mM $MgCl_2$, 25 mM NaCl, 20% glycerol, 21 mM BME) for a total 24 h at 4 °C, with one change of buffer after 12 h.

Protein preparation 2: Inclusion body production and on-column refolding

Escherichia coli strain BL21(DE3) transformed with pET28a-hPKM2 was grown in 1 L of LB-kan containing 5% (w/v) sucrose at 37 °C. The culture was induced at OD_{600} of 0.4 with 1 mM IPTG and shaking continued for 3 h at 37 °C. Following centrifugation, the cell pellet was resuspended in buffer G (50 mM Tris, pH 7.5, 100 mM KCl, 20% glycerol; 60 mL per 1 L culture) and lysed by sonication. Inclusion bodies were isolated by centrifugation at 15 000 ***g*** for 15 min, washed twice with inclusion body wash buffer 1 (50 mM Tris, pH 7.5, 10 mM EDTA, 2% Triton X-100, 500 mM NaCl, 5 mM DTT), once with inclusion body wash buffer 2 (50 mM Tris pH 7.5), and collected in a preweighed tube. The inclusion body pellet was resolubilized overnight at 4 °C in 1 mL of resuspension buffer (50 mM Tris, pH 8.0, 6 M guanidinium, 40 mM imidazole, 5 mM DTT) per 30 mg of wet pellet weight. A gravity flow column was packed with Ni-NTA beads (2 mL) at 22 °C and washed with four column volumes (CV) of resuspension buffer. Resolubilized protein was applied to the column and the column was washed with 15 CV of column wash buffer (50 mM Tris pH 8.0, 4 M urea, 40 mM imidazole, 1 mM DTT). To initiate refolding, the column was washed with 4 CV of refolding buffer (50 mM bis-tris propane, pH 8.0, 100 mM KCl, 20% glycerol, 2 mM $MgCl_2$). The column outlet was stopped and refolding continued at 22 ° C for 1 h. Protein was eluted using buffer H (50 mM bis-tris propane, pH 8.0, 100 mM KCl, 20% glycerol, 2 mM $MgCl_2$, 250 mM imidazole, 1 mM DTT). Fractions (1 mL) containing protein were pooled and DTT was added to a final concentration of 25 mM.

Protein preparation 3: Two-column purification of native proteins

Escherichia coli BL21(DE3) cells were transformed, induced, pelleted, and frozen as described in section 'Native protein expression' above. All protein purification steps were performed on ice or at 4 °C. The cell pellet from 1 L of culture was resuspended in a total of 60 mL buffer A (50 mM Tris, pH 7.5, 10 mM $MgCl_2$, 300 mM KCl, 10% glycerol, 5 mM imidazole) with protease inhibitors (Roche, Basel, Switzerland, 11836170001). Resuspended cells were lysed by sonication and the lysate was clarified by centrifugation at 20 000 ***g*** for 45 min. The supernatant was filtered using a 0.22-μm filter and applied to a Ni^{2+}-charged IMAC column (GE Healthcare HisTrap 1 mL; Chicago, IL, USA) using an Äkta FPLC system. The column was washed with 15 CV of wash buffer (50 mM Tris, pH 7.5, 10 mM $MgCl_2$, 300 mM KCl, 20 mM imidazole), then with 20 CV of wash buffer containing 20% elution buffer (50 mM Tris, pH 7.5, 10 mM $MgCl_2$, 250 mM KCl, 250 mM imidazole), and the protein was eluted with a 6 CV linear gradient from 20% to 100% elution buffer. Fractions containing the protein of interest were pooled and concentrated using Amicon Ultra centrifugal filters (Millipore, Burlington, MA, USA, UFC903024) and further purified by size-exclusion chromatography (GE Healthcare HiPrep 16/60, Sephacryl S-200) with buffer B (25 mM bis-tris propane, pH 7.5, 10 mM $MgCl_2$, 25 mM KCl) as the mobile phase. Fractions of interest were again pooled and spin-concentrated. Glycerol was added to the concentrated protein to 20% v/v,

concentration of purified PKM2 was determined by absorbance at 280 nm using an extinction coefficient of 29 910 $M^{-1}\cdot cm^{-1}$, and stored at −80 °C.

SDS/PAGE

Purified proteins were analyzed by SDS/PAGE using 8% polyacrylamide gels and visualized by Coomassie blue staining. Images of stained gels were obtained using a LI-COR Biosciences Odyssey imager.

Kinetic assays

A lactate dehydrogenase (LDH)-linked spectrophotometric assay was used to determine pyruvate kinase activity by measuring the oxidation of NADH *via* absorbance at 340 nm. The reaction buffer consisted of 50 mM bis-tris propane, pH 7.5, 200 mM KCl, 15 mM $MgCl_2$, 100 units per mL LDH, 2 mM ADP (or PEP), 180 μM NADH, and PEP (or ADP) concentrations from 0 to 2 mM as indicated. Enzymes were preincubated with or without 50 mM FBP prior to the start of the assay, and the reaction was initiated by adding reaction buffer to enzyme to a final volume of 100 μL in a well of a 96-well plate. Final FBP concentration was 5 mM when present in the assay. Final pyruvate kinase concentrations were chosen to allow measurement of initial rates; for example, wild-type enzymes were assayed at concentrations near 1 $\mu g\cdot mL^{-1}$. The reaction was monitored using a Tecan Infinite M200 Pro plate reader (Tecan Group Ltd., Männedorf, Switzerland). K_m and V_{max} values were calculated by fitting the initial rate data using GRAPHPAD PRISM software (GraphPad Software Inc., San Diego, CA, USA). One unit is defined as the amount of pyruvate kinase activity causing oxidation of one μmole of NADH per minute at 25 °C in the LDH-linked assay.

FBP activation assay

Enzymes were preincubated in various concentrations of FBP as indicated and the reaction initiated by the addition of reaction buffer containing the same FBP concentration. PEP concentrations were chosen to be insufficient to induce co-operativity. Apparent half-maximal effective concentration (EC_{50}) values for FBP binding were determined by fitting the data to a sigmoid dose–response curve with variable slope using GRAPHPAD PRISM software.

Size-exclusion chromatography

About 5 μg of wild-type and mutant PKM2 proteins in a volume of 10 μL were subjected to HPLC separation on a Yarra SEC-3000 size-exclusion column (Phenomenex, Torrance, CA, USA) with an aqueous mobile phase containing 25 mM bis-tris propane, pH 7.1, 25 mM KCl, and 10 mM $MgCl_2$ at a flow rate of 1 $mL\cdot min^{-1}$. The proteins used in this assay were prepared using Protein Preparation 3 and were assayed in the absence of FBP.

Results

Kinetic characterization of PKM2 and PKM1

Including a 6x-histidine tag on proteins facilitates purification using Ni-affinity chromatography, and the kinetic parameters of PKM2 are not altered by a 6x-histidine tag [15]. To determine whether single-step Ni-affinity could be used to prepare recombinant PKM2 proteins for kinetic analysis, 6x-His-PKM2 expressed in *E. coli* was isolated from bacterial lysates *via* binding to Ni-NTA beads, single-step elution with imidazole, and followed by dialysis as reported previously [20,29,38]. 6x-His-PKM2 prepared using this one-step protocol (Protein Preparation 1 in Experimental Methods; hereafter 'Prep 1') was active and exhibited hyperbolic kinetics with respect to PEP substrate; however, addition of the allosteric activator FBP to the reaction did not substantially increase affinity for PEP or increase the maximal velocity of the enzyme (Fig. 1A). These results suggested that most of the enzyme was already bound to FBP from the bacteria despite purification as previously reported [19,23,39]. Independent preparations of PKM2 using this approach occasionally produced enzyme that showed some FBP activation; however, this variability in FBP activation complicated detailed kinetic analysis. Ammonium sulfate precipitation has been previously used to remove allosteric effectors from liver pyruvate kinase preparations [40,41], as sulfate ions appear to interfere with the interaction between FBP and the liver enzyme [41]. The inclusion of 300 mM ammonium sulfate in the kinetic assay allowed for the observation of FBP activation when PKM2 prepared in this manner was studied (Fig. 1B). In the presence of ammonium sulfate, FBP increased the affinity of the enzyme for PEP without affecting V_{max}, suggesting that the PKM2 tetramer is incompletely saturated with bacterially derived FBP under these conditions. In order to analyze PKM2 that was not bound to bacterial FBP, unfolded 6x-histidine-tagged PKM2 was isolated in the form of bacterial inclusion bodies, washed extensively in a denatured state incapable of binding FBP, and then refolded in the absence of FBP using an on-column refolding protocol (Protein Preparation 2 in Experimental Methods; hereafter 'Prep 2'). PKM2 prepared using Prep 2 exhibited activation by FBP, as evidenced by a decrease in apparent K_m for PEP and an increase in V_{max} (Fig. 1C). The observed increase in V_{max} is consistent with an FBP-induced assembly of fully

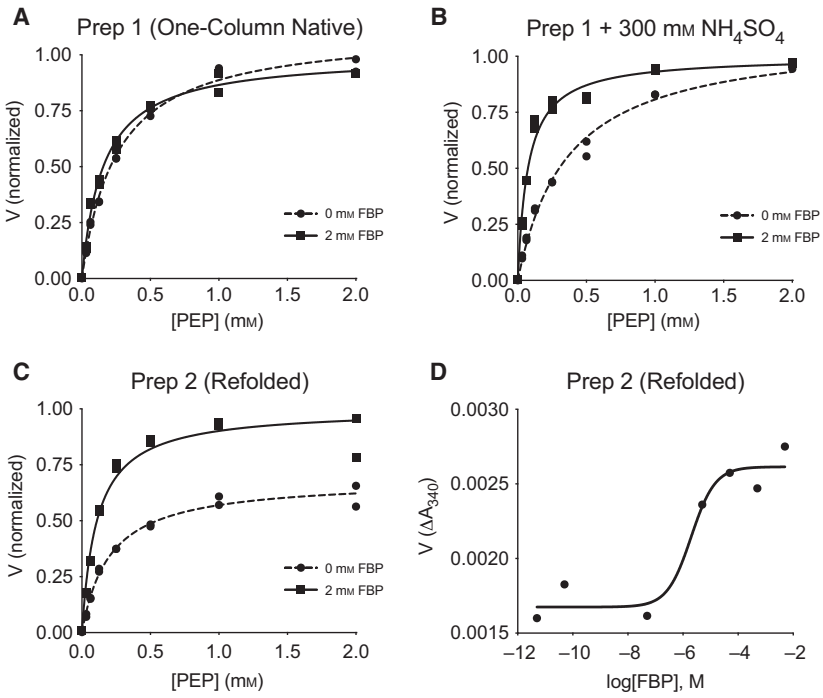

Fig. 1. Steady-state kinetics and FBP activation of 6x-His-PKM2 prepared using different approaches. Individual data points are plotted, and assays were conducted using a saturating ADP concentration (5 mM) and the indicated concentration of FBP. (A) PKM2 reaction rate (V) with respect to PEP concentration for the enzyme purified using one-step Ni-NTA affinity chromatography (Prep 1). (B) Reaction rate (V) with respect to PEP concentration for Prep 1 PKM2 in the presence of 300 mM ammonium sulfate. (C) Reaction rate (V) with respect to PEP concentration for PKM2 isolated from inclusion bodies and refolded in the absence of FBP (Prep 2). (D) Activation of refolded Prep 2 PKM2 by FBP in the presence of subsaturating (0.125 mM) PEP and saturating (5 mM) ADP.

active PKM2 tetramers and is consistent with previous studies [7,16]. An activity-based determination of FBP activation of refolded PKM2 protein yielded an AC_{50} value of ~ 2 μM (Fig. 1D), which is also comparable to previously reported values for PKM2 activation [7] and binding of FBP to nonphosphorylated PKL [41], although somewhat higher than a more recently reported AC_{50} of 118 nM [19]. Despite the kinetic behavior of the refolded PKM2 in response to FBP being more consistent with past studies, Prep 2 was laborious and we sought an alternative preparation of native, bacterially expressed PKM2 that is largely free of bacterial FBP.

Ni-affinity chromatography followed by size-exclusion chromatography of soluble 6x-His-tagged PKM2 allowed the isolation of FBP-responsive PKM2 with high specific activity (Fig. S2). PKM2 protein prepared *via* this method (Protein Preparation 3 in Experimental Methods; hereafter 'Prep 3') retained the ability to be activated by FBP, and similar to refolded FBP-free PKM2 generated using Prep 2, FBP caused an increase in V_{max} and a reduction in K_m with respect to PEP (Fig. 2A). FBP had little effect on K_m with respect to ADP for protein produced in this manner (Fig. 2B). The qualitative similarity between kinetics of refolded PKM2 (Prep 2) and PKM2 that was prepared using two-column purification (Prep 3) suggests that the addition of size-exclusion chromatography is sufficient to separate PKM2 from the FBP present in the bacterial lysate. We also observed little variation in enzyme qualities when PKM2 was independently purified using the two-column Prep 3 (Fig. S3). As expected, PKM1 protein prepared using Prep 3 exhibited hyperbolic kinetics with respect to PEP and was not activated by FBP (Fig. 2C,D). These results are summarized in Table 1, and the kinetic behavior of PKM2 and PKM1 is consistent with that reported previously, including a requirement for FBP to improve PKM2 catalytic function [7,15]. Of note, the slightly lower V_{max} observed for PKM1 compared to FBP-activated PKM2 should not be interpreted as PKM1 being an inferior enzyme. These results also establish Prep 3 as a method for preparing mutant enzymes to study how mutations affect the kinetic parameters of PKM2.

Mutations in PKM2 found in human cancer

Mis-sense mutations throughout the coding sequence of PKM2 were found from sequencing of primary human cancers [29]. To determine whether cancer-associated mutations found in the TCGA occurred in conserved residues, the protein sequences of pyruvate kinase isoforms from various species were aligned and the locations of all 23 mutations identified in human cancers were compared to residues found in other pyruvate kinase proteins (Fig. 3). More than half (13/23) of the mutations were found in residues that were identical across all pyruvate kinase proteins

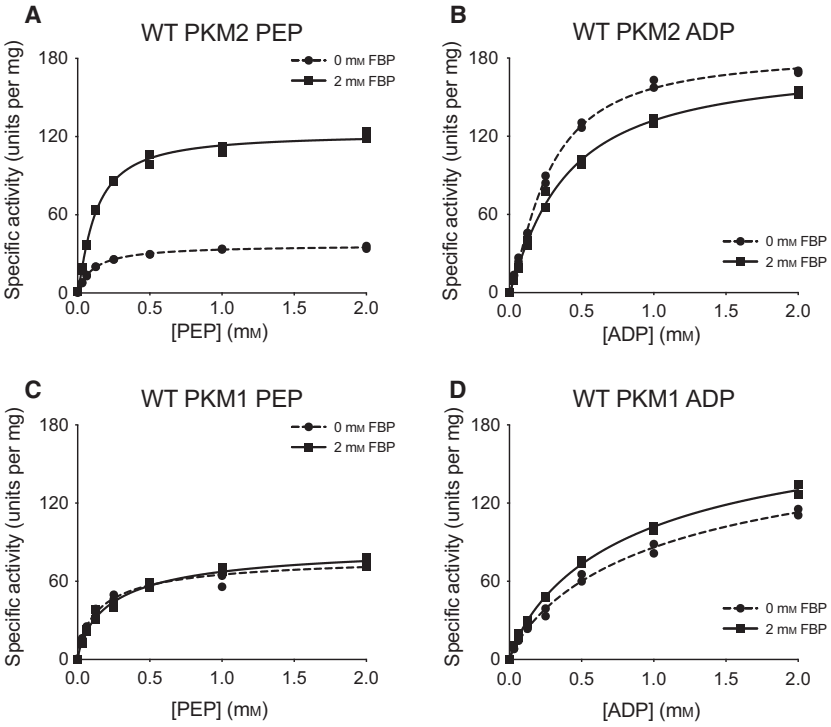

Fig. 2. Steady-state kinetics of 6x-His-PKM2 and 6x-His-PKM1 prepared using two-column purification (Prep 3). All conditions were performed in duplicate using proteins prepared with Prep 3, and individual data points are shown. (A) PKM2 activity with varying concentrations of PEP and saturating (5 mM) ADP. (B) PKM2 activity with varying concentrations of ADP and saturating (5 mM) PEP. (C) PKM1 activity with varying concentrations of PEP and saturating (5 mM) ADP. (D) PKM1 activity with varying concentrations of ADP and saturating (5 mM) PEP.

considered, suggesting that many of these residues may be important for enzyme function.

The P117L, R246S, G415R, R455Q, and R516C cancer mutants were selected for study because they were examples of mutations from a variety of enzyme locations (Fig. S4). These mutations were among the first identified by the TCGA in the human *PKM* gene, and they occurred at low frequency in a variety of tumors, including uterine, kidney, and lung adenocarcinoma (Table S1). These PKM2 mutants were prepared using the two-column purification (Prep 3) procedure, and enzyme kinetics were determined with respect to PEP and ADP (Figs 4 and 5). A functional FBP activation assay was also used to determine FBP AC_{50} values for WT, P117L, R246S, G415R, and R455Q (Fig. 6A–E). Given the relatively low enzyme concentrations required for activity-based assays, the response to FBP during AC_{50} determination is likely a factor of both FBP binding affinity and the tetramer-monomer equilibrium in solution [18], either of which may be affected by mutations. The location of the mutations and the effects on PKM2 function are described below.

P117 is found in the 'hinge' region of the protein between the A and B domains that allows closure of the active site upon substrate binding (Fig. S5); P117 is conserved from humans to *E. coli*. Despite a reduction in overall velocity, the P117L mutant retains near wild-type affinity for PEP in the presence and absence of FBP, and the enzyme appears capable of forming stable tetramers in response to FBP binding as addition of FBP increases enzyme V_{max} (Fig. 4A,B). The main effect of the P117L substitution is to greatly reduce the affinity of the enzyme for ADP (Fig. 5A). The K_m with respect to ADP increased by a factor of 4 to 5, to 1.84 mM in the absence of FBP and 1.93 mM in the presence of FBP (Table 2). These data suggest that FBP acts on this PKM2 mutant to stabilize a tetrameric form of the enzyme despite its reduced ADP affinity. The P117L mutation has some effect on apparent FBP activation, as the AC_{50} for FBP is increased relative to wild-type PKM2 (Fig. 6A,B). Interestingly, a large selective reduction of ADP binding affinity has been observed in the R119C mutant of PKM1 [42]. R119 also lies near the hinge region and the active site cleft; however, the positive side chain of R119 is exposed in the active site and may play a more direct role in ADP binding than does P117.

R246 is partially solvent-exposed and is part of the TIM barrel of the enzyme A domain, and is located within 14 angstroms of the active site (Fig. S6). In the wild-type protein, the R246 side chain appears to hydrogen bond with the backbone oxygen of F244 and form an electrostatic interaction with the negatively charged side chain of D250. The R246S mutant displays a reduction in overall specific activity and a decrease in affinity for PEP relative to wild-type

Table 1. Kinetic parameters for PEP in the presence and absence of 2 mM FBP for wild-type and mutant PKM2.

Enzyme	FBP	K_m (μM)	V_{max} (U·mg^{-1})	V_{max} Normalized	n_H	Fit[a]/R^2	FBP AC_{50} (95% CI)
PKM2 Prep 1	–	254.5 ± 18.02		111%[b]	(1.0)	M/0.9934	
	+	155.8 ± 12.80		100%[b]	(1.0)	M/0.9908	
PKM2 Prep 1 +	–	360.2 ± 33.56		110%[b]	(1.0)	M/0.9904	
300 mM $(NH_4)_2SO_4$	+	74.08 ± 6.798		100%[b]	(1.0)	M/0.9862	
PKM2 Prep 2	–	202.7 ± 17.49	94.82 ± 2.466	68.5%[b]	(1.0)	M/0.9898	
	+	109.5 ± 14.38	138.4 ± 4.694	100%[b]	(1.0)	M/0.9739	1.98 μM (0.207–18.9)
PKM1 Prep 3	–	126.6 ± 13.76	73.45 ± 2.134	90.8%[b]	(1.0)	M/0.9813	
	+	191.2 ± 19.46	80.74 ± 2.441	100%[b]	(1.0)	M/0.9849	
PKM2 Prep 3	–	109.1 ± 3.787	36.92 ± 0.3305		(1.0)	M/0.9981	48.7 nM (8.46–281)
	+	141.4 ± 9.801	129.5 ± 2.472		(1.0)	M/0.9929	
PKM2 P117L	–	171.0 ± 18.34	30.07 ± 1.260		1.4 ± 0.56	H/0.9837	2.37 μM (0.567–9.77)
	+	173.2 ± 21.34	74.84 ± 3.275		0.97 ± 0.11	H/0.9898	
PKM2 R246S	–	517.8 ± 90.46	57.13 ± 6.216		2.1 ± 0.56	H/0.9514	788 nM (102–6111)
	+	194.2 ± 33.39	94.74 ± 5.651		0.97 ± 0.11	H/0.9858	
PKM2 G415R	–	1124 ± 140.3	82.68 ± 6.323		1.4 ± 0.10	H/0.9977	
	+	3170 ± 2219	234.8 ± 94.16		0.99 ± 0.12	H/0.9915	
PKM2 R455Q	–	404.6 ± 75.60	172.7 ± 11.91		0.93 ± 0.08	H/0.9927	693 nM (398–1208)
	+	129.3 ± 4.126	161.3 ± 1.837		1.2 ± 0.004	H/0.9988	
PKM2 R516C	–	128.7 ± 18.62	10.51 ± 0.4431		0.72 ± 0.06	H/0.9953	
	+	177.5 ± 17.98	10.91 ± 0.3963		1.1 ± 0.09	H/0.9928	
PKM2 S37A	–	853.1 ± 377.6	148.4 ± 21.71		0.71 ± 0.08	H/0.9917	
	+	144.6 ± 9.667	159.4 ± 3.964		1.3 ± 0.09	H/0.9940	
PKM2 K270M	–	101.5 ± 37.25	5.144 ± 0.6810		1.5 ± 0.70	H/0.7595	
	+	68.01 ± 17.26	6.253 ± 0.5325		1.2 ± 0.40	H/0.8954	
PKM2 K367M	–	299.2 ± 71.17	43.72 ± 3.717		0.94 ± 0.12	H/0.9832	
	+	85.89 ± 6.838	33.03 ± 0.8520		1.4 ± 0.15	H/0.9893	
PKM2 R399E	–	503.8 ± 97.94	84.90 ± 6.284		0.93 ± 0.08	H/0.9936	
	+	158.8 ± 13.71	115.8 ± 3.784		1.3 ± 0.12	H/0.9905	
PKM2 K433E	–	739.5 ± 338.8	94.12 ± 14.63		0.75 ± 0.09	H/0.9881	
	+	137.1 ± 9.522	85.26 ± 2.071		1.1 ± 0.07	H/0.9958	
PKM2 H464A	–	804.8 ± 69.91	139.2 ± 8.135		1.9 ± 0.17	H/0.9947	
	+	88.53 ± 4.996	113.8 ± 2.243		1.3 ± 0.10	H/0.9937	

[a] Substrate-velocity data were fit using Michaelis–Menten (M) or Hill (H) models.; [b] Maximum velocities relative to the FBP condition.

(Fig. 4B). The disruption of catalytic efficiency of the enzyme is likely due to changes in active site conformation caused by disruption of the tertiary structure through the loss of structural interactions in the A domain. This mutation had little effect on ADP and apparent FBP activation (Figs 5B and 6C).

G415 is located at the dimer-dimer interface of the tetramer. This glycine is located on an α-helix at the subunit interface and positioned such that the G415 of one subunit is in contact with the G415 of the subunit on the opposite side of the interface (Fig. S7). The lack of a bulky side chain allows tight packing of the α-helices at the interface. The G415R substitution introduces a large, charged residue at this interface and appears to abolish FBP activation of the enzyme (Figs 4C, 5C and 6D). PKM2 G415R exhibits co-operativity with respect to PEP binding in the absence of FBP (n_H = 1.4), and this co-operativity is reduced in the presence of FBP (n_H = 0.99). The reduction of co-operativity and V_{max} increase caused by FBP suggest that FBP does indeed bind to the enzyme, but the G415R mutation blunts FBP activation to levels that may not be physiologically meaningful.

R455 is located near the FBP-binding pocket and forms intrachain electrostatic contacts with D476 and D485 (Fig. S8). Loss of charge due to the R455Q substitution might be expected to disrupt the tertiary structure and affect FBP binding. This mutation appears to slightly decrease affinity for ADP and increase the apparent FBP AC_{50} to 693 nM, but the R455Q mutant otherwise retains near wild-type activity (Figs 4D, 5D and 6E).

R516 is located on the FBP binding loop of the enzyme, but this residue is solvent-exposed and does not make contact with other parts of the protein or bound FBP (Fig. S9). Interestingly, the R516C

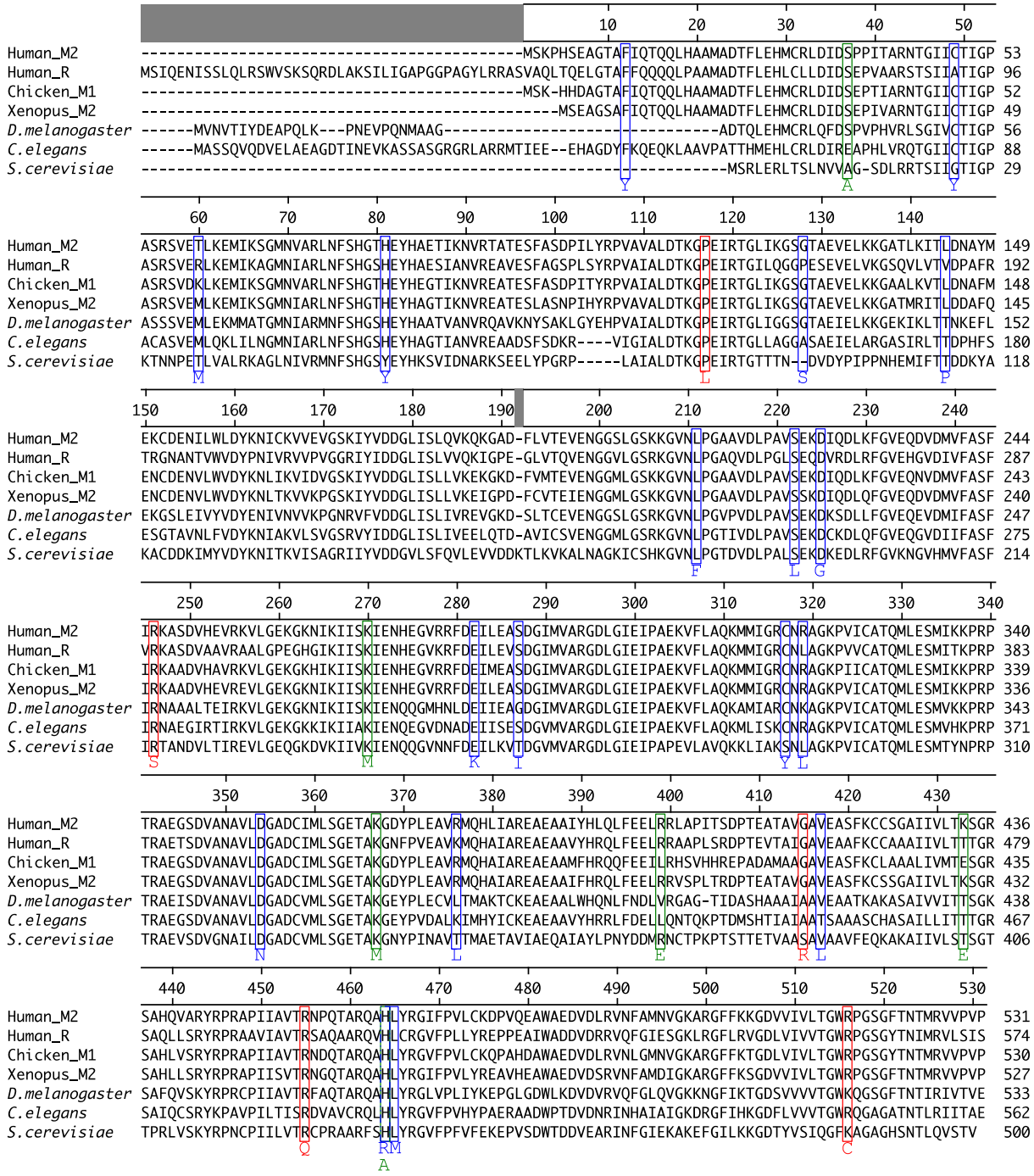

Fig. 3. Multiple sequence alignment of pyruvate kinase isoforms from different species. The locations of mutations found in human tumors [29] are marked with blue or red boxes. The red boxes indicate the mutations characterized in this study. Green boxes mark residues mutated in past studies of PKM2 function [17,23,35,36,43] that were characterized in this study.

mutation greatly reduces the catalytic efficiency of the enzyme for unclear reasons (Figs 4E and 5E).

A summary of kinetic parameters is provided in Tables 1 and 2. Overall, the PKM2 mutants identified in human cancers that were evaluated exhibited either lowered maximal activity or reduced affinity for substrates and/or FBP when compared to wild-type PKM2.

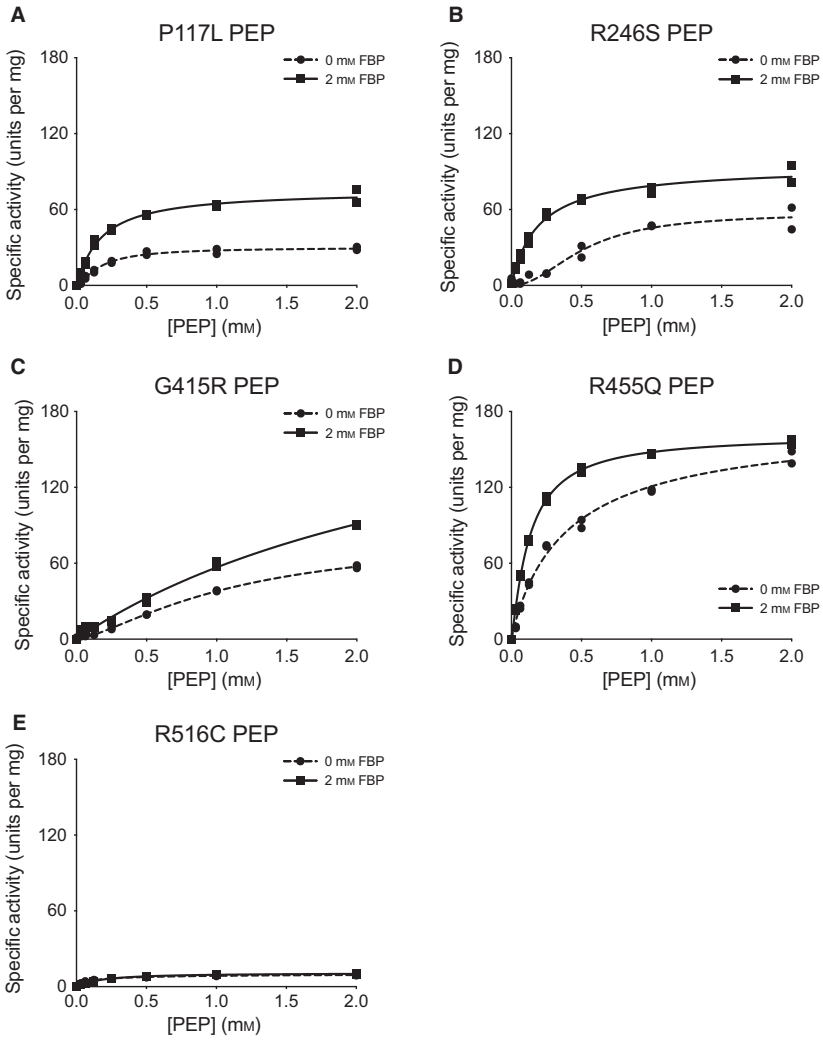

Fig. 4. Steady-state kinetics of PKM2 cancer mutants with respect to PEP concentration. All proteins were prepared using Prep 3. For each indicated mutant, the ADP concentration was held constant at 2 mM. Assays were performed in duplicate and all data points are shown with allosteric sigmoidal (Hill) fit lines.

Mutations in PKM2 generated to study enzyme functions

Several studies have introduced mutations into PKM2 in an attempt to abolish nonglycolytic aspects of protein function, or to alter the response of the enzyme to allosteric effectors [17,23,35,36]. The effects of these mutations on the kinetic parameters of PKM2 as a glycolytic enzyme have not been extensively characterized. The substitutions considered here include S37A, K367M, K270M, R399E, K433E, and H464A [17,23,35,36,43,44]. These mutant enzymes were prepared using two-column purification (Prep 3), and all enzymes were assayed for kinetics with respect to PEP and ADP in the absence and presence of FBP (Figs 7A–F and 8A-F).

Phosphorylation of PKM2 on S37 is reported to facilitate translocation of PKM2 to the nucleus for a role in oncogenic signaling [36]. The S37A mutation eliminates phosphorylation at S37 and reduces orthotopic xenograft growth of glioblastoma cells in mice. In the absence of added FBP, PKM2 S37A exhibited an increase in the K_m for PEP (Table 1) and a reduction in V_{max} with respect to ADP (Table 2) when compared to wild-type PKM2, indicating that the S37A mutation may affect activity of the enzyme despite being solvent-exposed and relatively far from ligand-binding sites (Fig. S10).

The K367M mutation was generated in an effort to disrupt the predicted ADP-binding site of PKM2 and generate a kinase-inactive mutant [43]; however, the functional effect of this amino substitution was never assessed for the human enzyme. Inspection of the ADP-bound PKM2 crystal structure shows that K367 is indeed near the active site (Fig. S11), but the side chain does not make direct contact with the bound substrate (Fig. S12). While the K367M mutation does decrease specific activity and affinity for both PEP and

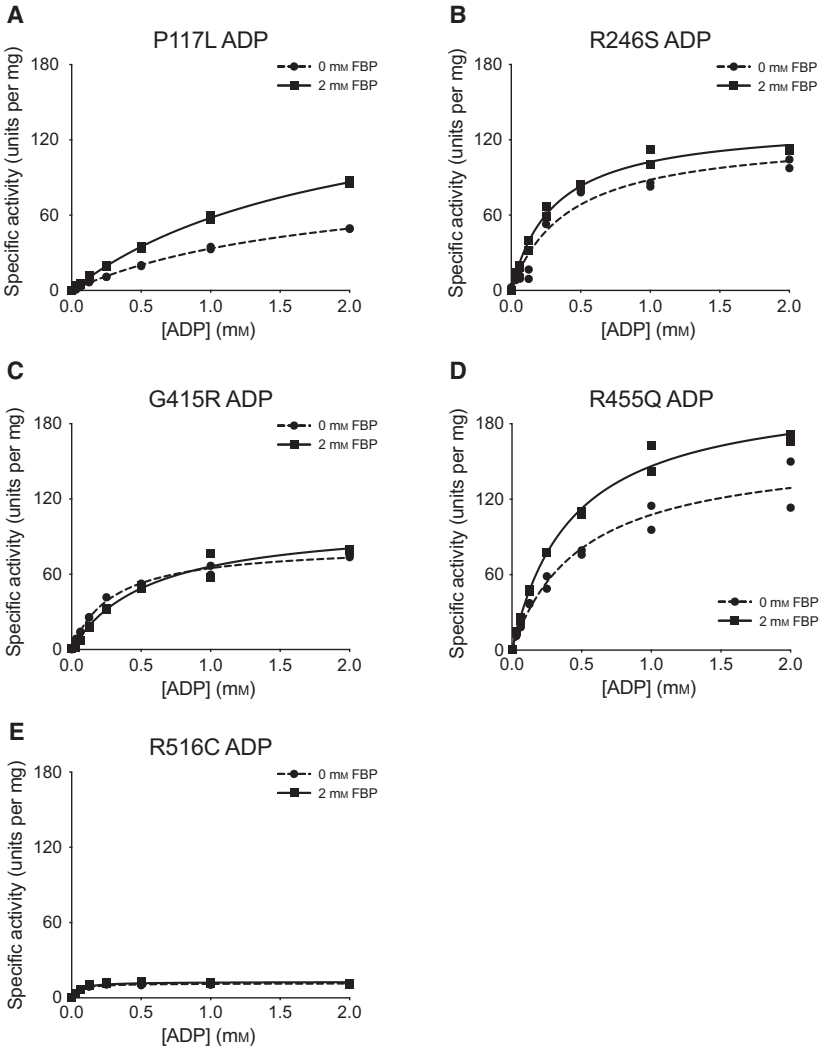

Fig. 5. Steady-state kinetics of PKM2 cancer mutants with respect to ADP concentration. All proteins were prepared using Prep 3. For each indicated mutant, the PEP concentration was held constant at 2 mM. Assays were performed in duplicate and all data points are shown with Michaelis–Menten fit lines.

ADP, the mutant still retains some activity with V_{max} about 30% that of the wild-type enzyme (Figs 7B and 8B). These findings are similar to those reported for this mutation at a single set of substrate conditions [45]. Because the K367M substitution does not fully abolish PKM2 enzymatic activity, caution is advised in interpreting studies that rely on this mutation as completely disrupting PKM2 catalytic function for the pyruvate kinase reaction [43,45–48].

An alternative catalytically dead mutant of PKM2 can be generated by introducing a K270M mutation [44]. K270 is a catalytic lysine in the enzyme active site (Fig. S11) that serves to stabilize the pentacoordinate transition state that forms during the transfer of phosphate between reactant and product [15]. Substitution of the analogous lysine in *Saccharomyces cerevisiae* (K240) and *Bacillus stearothermophilus* (K221) with methionine results in properly folded enzymes with severely reduced catalytic activity [49,50]. The activity of the yeast K240M mutant is reduced by approximately 1000-fold when using Mg^{2+} as a cofactor [49]. Testing the effect of introducing this mutation into the human enzyme demonstrates that a K270M mutation reduces the overall activity of hPKM2 to less than 5% of the wild-type enzyme (Figs 7C and 8C). Both the K270M and K367M mutants can be produced *via* Prep 3 with similar yield and purity when compared with wild-type PKM2 (Fig. S13).

The R399E mutation results in the loss of intersubunit contacts across the dimer-dimer interface (Fig. S14), and has been reported to be a constitutive dimer with enhanced protein kinase activity [35], although a later study suggested that the R399E mutant can indeed form tetramers [51]. PKM2 R399E exhibits increased co-operativity with respect to PEP (n_H = 1.3) in the absence of FBP when compared to

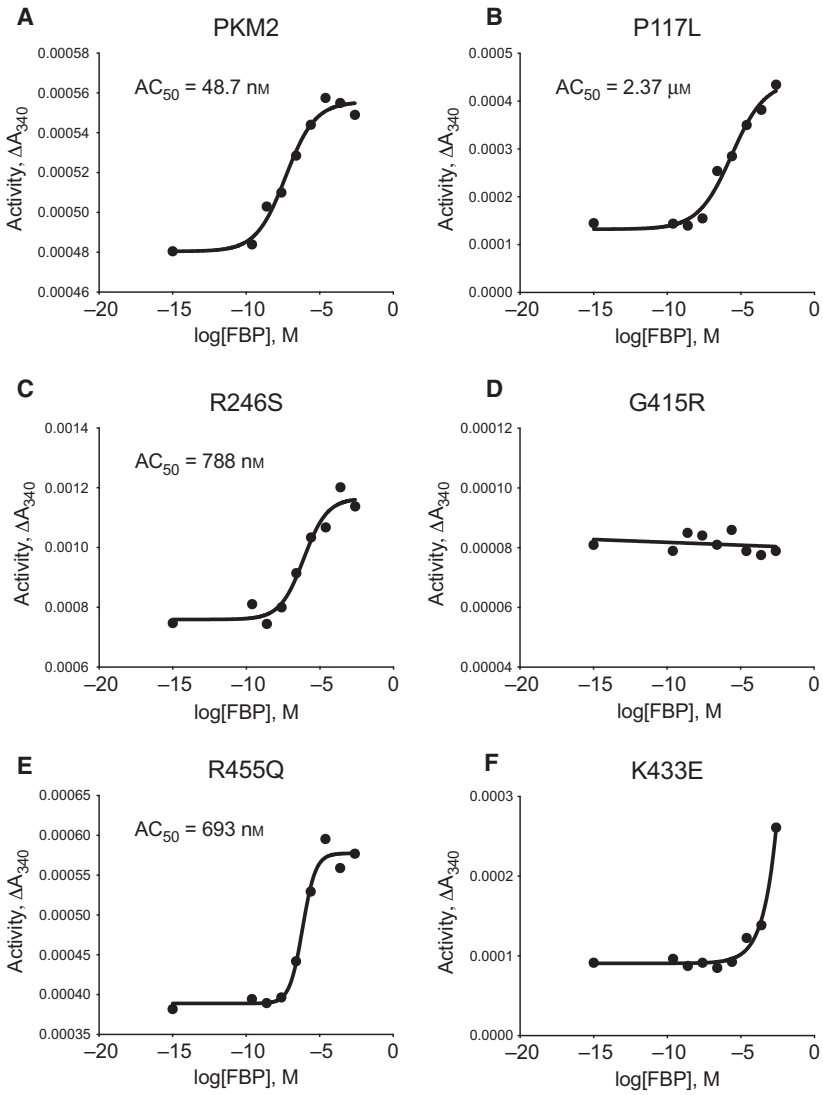

Fig. 6. Activation of PKM2 and PKM2 cancer mutants by FBP. All proteins were prepared using Prep 3. For each indicated mutant, activity was assessed with 2 mM ADP and 0.125 mM PEP and data points are means of duplicate measurements. Data were fit to a sigmoid dose–response curve with variable slope, except that G415R was fit with linear regression.

wild-type PKM2 (Table 1). FBP increases affinity of the R399E mutant enzyme for PEP but not ADP, as evidenced by a large decrease in the K_m for PEP (Tables 1 and 2; Figs 7D and 8D). In addition to the effect of FBP on PEP binding affinity, V_{max} for PEP increases somewhat during FBP activation (Fig. 7D, Table 1), suggesting tetramer assembly or stabilization in the active state.

K433 is located on a loop that forms part of the FBP-binding pocket (Fig. S15). This positively charged residue is reported to interact with phosphotyrosine residues on other proteins during intracellular signaling and facilitate the inactivation of PKM2 by causing the release of the allosteric activator FBP [23]. The K433E substitution has been reported to interfere with phosphotyrosine-based FBP release, but not with FBP activation of the protein. PKM2 K433E was responsive to activation by FBP (Figs 6F, 7E and 8E). FBP increased affinity for PEP as evidenced by a decrease in K_m with respect to PEP; however, the mutant enzyme shows a somewhat reduced V_{max} with FBP as compared to the wild-type enzyme (Table 1). Additionally, the affinity of the enzyme for FBP appears to be reduced relative to wild-type PKM2, as shown by the effect of FBP titration on enzyme activity (Fig. 6F).

Serine acts as an allosteric activator of PKM2 with a reported AC_{50} of 1.3 mM [17], and H464 is found in the serine/alanine/phenylalanine binding pocket (Fig. S16) [7,17,52]. Substitution of H464 with alanine is reported to abolish serine binding without affecting FBP activation [17]. Our results confirm that PKM2 H464A is activated by FBP (Figs 7F and 8F). When compared to wild-type enzyme, the H464A mutation

Table 2. Michaelis–Menten kinetic parameters for ADP in the presence and absence of 2 mM FBP for wild-type and mutant PKM2.

Enzyme	FBP	K_m (μM)	V_{max} (U·mg^{-1})	R^2
PKM2 (Prep 3)	–	364.6 ± 33.20	209.6 ± 6.740	0.9909
	+	453.6 ± 29.40	189.8 ± 4.630	0.9957
PKM1	–	744.4 ± 62.40	153.1 ± 5.628	0.9940
	+	623.7 ± 37.24	168.4 ± 4.168	0.9967
PKM2 P117L	–	1836 ± 132.7	94.74 ± 4.013	0.9978
	+	1932 ± 109.0	169.6 ± 5.699	0.9987
PKM2 R246S	–	406.4 ± 90.97	124.0 ± 10.12	0.9511
	+	302.9 ± 26.98	133.5 ± 3.987	0.9905
PKM2 G415R	–	294.1 ± 20.84	83.96 ± 1.891	0.9949
	+	558.6 ± 81.54	103.2 ± 5.989	0.9820
PKM2 R455Q	–	495.7 ± 87.61	161.0 ± 10.99	0.9683
	+	426.7 ± 32.36	208.7 ± 5.848	0.9938
PKM2 R516C	–	45.75 ± 6.187	11.64 ± 0.3176	0.9718
	+	50.34 ± 9.253	12.82 ± 0.4903	0.9492
PKM2 S37A	–	338.0 ± 36.89	87.31 ± 3.294	0.9858
	+	459.4 ± 61.19	157.1 ± 7.904	0.9816
PKM2 K270M	–	275.7 ± 47.84	6.063 ± 0.3438	0.9644
	+	185.7 ± 72.53	5.909 ± 0.7172	0.8012
PKM2 K367M	–	274.7 ± 30.90	45.47 ± 1.670	0.9844
	+	297.4 ± 24.85	28.31 ± 0.7892	0.9911
PKM2 R399E	–	513.1 ± 34.49	172.5 ± 4.515	0.9956
	+	657.1 ± 71.43	166.4 ± 8.336	0.9903
PKM2 K433E	–	444.0 ± 80.40	113.8 ± 7.702	0.9656
	+	713.5 ± 31.26	191.6 ± 3.632	0.9984
PKM2 H464A	–	456.9 ± 36.59	138.6 ± 4.185	0.9933
	+	612.2 ± 42.74	213.1 ± 6.132	0.9957

reduces V_{max} in the FBP-bound state and increases the co-operativity of PEP binding in the absence of FBP.

A summary of kinetic parameters for the engineered mutants studied is also provided in Tables 1 and 2. While each cancer mutation and engineered mutant has a unique effect on enzyme kinetics, one theme that emerges is that these amino acid substitutions often reduce the apparent affinity of PKM2 for PEP compared to wild-type enzyme, especially in the absence of FBP. This pattern is evident in Table 1, as 7 of 11 mutants exhibit a twofold or greater increase in the K_m for PEP compared to wild-type when FBP is absent.

Effect of mutations on tetramer-monomer equilibrium

We sought to determine the effect of mutations on the ability of PKM2 mutants to form stable tetramers when prepared *via* Prep 3 and assayed without exogenous FBP. HPLC-based size-exclusion chromatography showed that wild-type PKM2 formed stable tetramers under our separation conditions (Fig. 9). This HPLC separation method allows injection of enzyme at a relatively high concentration of 0.5 mg·mL^{-1}, which is approximately 500-fold more concentrated than enzyme concentrations used for the kinetic assays. This provides an equivalent concentration of monomers (~ 86 μM) that is almost two orders of magnitude greater than the recently reported tetramer-dimer and tetramer-monomer dissociation constants of around 1 μM for wild-type PKM2 [18,39]. The nondilutive HPLC assay conditions should thus favor PKM2 tetramer formation and provide a more direct measure of tetramer stability than the functional AC_{50} determinations. Interestingly, most mutants separated on size-exclusion chromatography as tetramers using this assay, with the exception of G415R and R399E. The G415R mutation is expected to disrupt the packing of α-helices at the dimer-dimer interface of the tetramer (Fig. S7), and this mutant protein eluted at a time consistent with it being predominantly a monomer. The R399E mutant enzyme mostly eluted as a tetramer; however, some protein eluted at a volume consistent with a dimer, consistent with the loss of intersubunit contacts across the dimer-dimer interface in this mutant (Fig. S14) only partially disrupting tetramer formation in these relatively concentrated conditions. Taken together, these results imply that most PKM2 mutations studied may have less effect on the

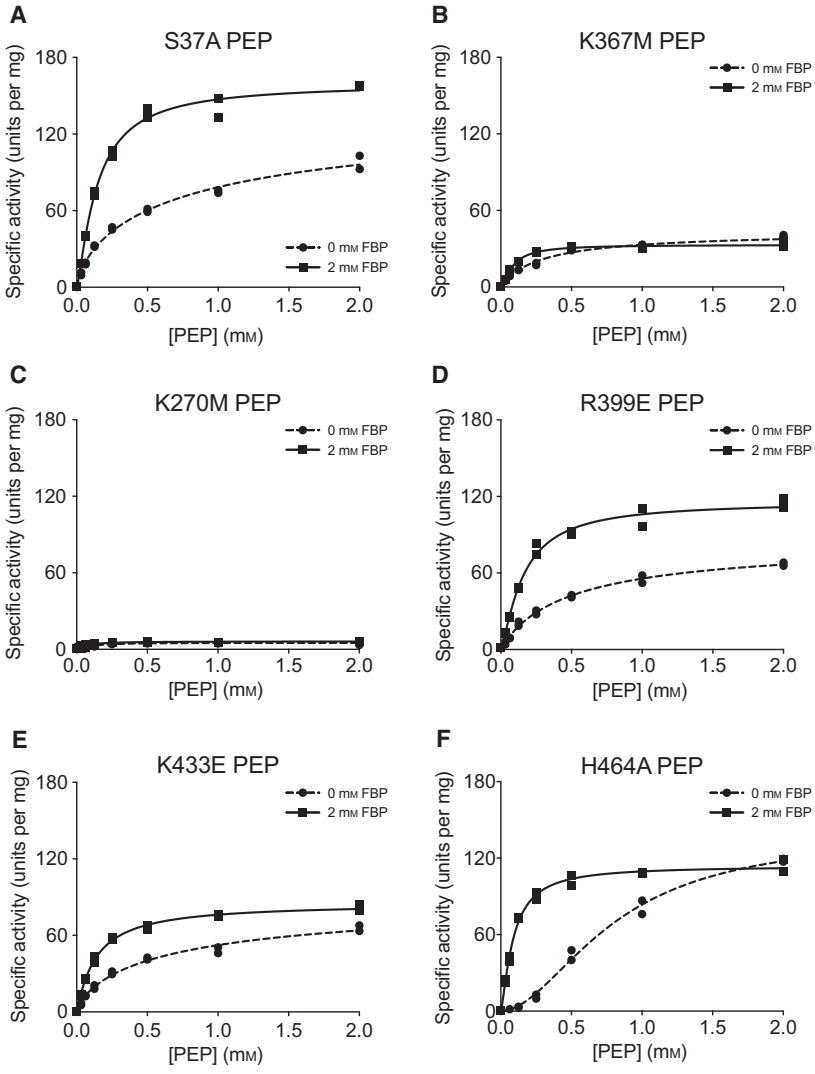

Fig. 7. Steady-state kinetics of PKM2 'Literature' mutants with respect to PEP concentration. All proteins were prepared using Prep 3. For each indicated mutant, activity was assessed with ADP concentration held constant at 2 mM. Assays were performed in duplicate and all data points are shown with allosteric sigmoidal (Hill) fit lines.

tetramer-monomer equilibrium *in vivo* than suggested by the steady-state kinetics or FBP AC_{50} values.

Discussion

Single amino acid substitutions affecting PKM2 are found in human cancers, and the mutations considered in this study tended to lower affinity of the enzyme for substrate, reduce its maximal activity, or alter activation by FBP. That these mutations have functional effects is not surprising for two reasons. First, these mutations affect residues that are highly conserved, and many of the cancer mutations considered here are located near functional sites on the enzyme. Second, PKM2 activity was found to be sensitive to amino acid substitution when SNPs in the human population that lead to PKM2 mis-sense mutations were studied and found to result in reduced enzyme activity, reduced thermal stability, or altered allosteric regulation [32]. Characterization of mis-sense PKM2 mutations in patients with Bloom syndrome, the underlying cause of which is defective DNA damage repair, revealed that the mutations studied also negatively affect PKM2 function [53–55].

The high affinity of PKM2 for FBP is shared by other mammalian pyruvate kinase isoforms such as PKL, but not by the pyruvate kinase isoforms of unicellular organisms. The values reported elsewhere for half-maximal binding or half-maximal activation of mammalian pyruvate kinases are in the sub- to low-micromolar range (0.34–7.5 μM) [7,39,41], with the most recent work reporting K_D = 25.5 nM for direct binding of FBP to PKM2 (after correction for copurified FBP) and AC_{50} = 118 nM for FBP activation of wild-type PKM2 [19]. While the FBP AC_{50} value reported in the present study for WT PKM2 (48.7 nM,

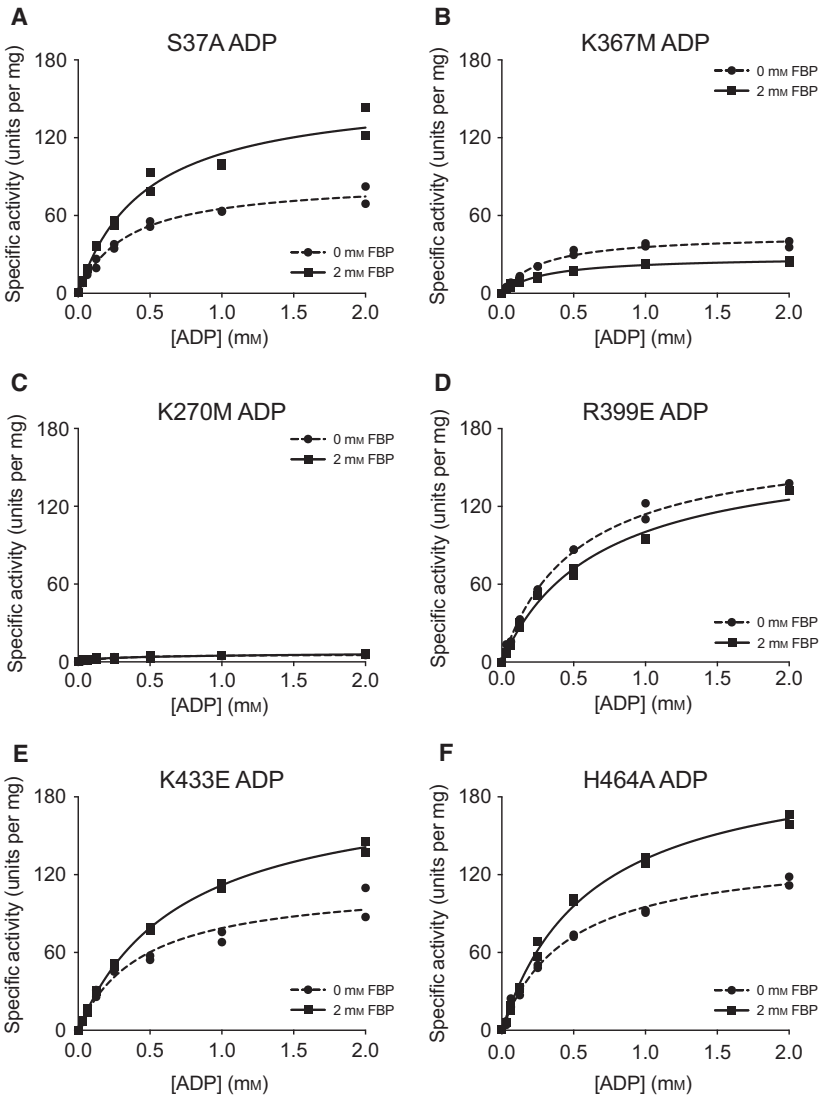

Fig. 8. Steady-state kinetics of PKM2 'Literature' mutants with respect to ADP concentration. All proteins were prepared using Prep 3. For each indicated mutant, activity was assessed with PEP concentration held constant at 2 mM. Assays were performed in duplicate and all data points are shown with Michaelis–Menten fit lines.

Fig. 6A and Table 1) compares favorably to those values, the FBP AC_{50} values we observe for refolded PKM2 is higher (1.98 μM), although still within the range of previously reported results. While this discrepancy may be an artifact of the preparation methods, there is greater imprecision in the AC_{50} parameter for refolded PKM2. A reported value for the intracellular FBP concentration in mammalian cells is 80 μM [56], which is at least one order of magnitude greater than the concentration required for half-maximal activation of PKM2. Thus, in the absence of other inputs, FBP binding to mammalian pyruvate kinases may be saturated in many cellular conditions *in vivo* [19]. In contrast, the $K_{0.5}$ values for FBP activation are around 45 μM for *S. cerevisiae* pyruvate kinase [57] and 70 μM for *E. coli* pyruvate kinase [58], making the yeast and *E. coli* pyruvate kinase isoforms better suited to respond to changes in intracellular FBP occurring in the physiological concentration range. Estimates of FBP concentration in *E. coli* and yeast can be higher than those found in mammalian cells [59,60], arguing that FBP concentrations can be high enough to saturate the microbial enzymes under some conditions. The mammalian isoforms appear to have traded some allosteric control based on FBP concentration for regulation by intracellular signaling to control metabolism in different specialized tissue contexts. Inactivation of PKL by phosphorylation during gluconeogenesis in the liver is one example, and inactivation of PKM2 due to FBP release caused by growth signaling in proliferating cells is another.

Most wild-type and mutant PKM2 protein eluted at a volume consistent with tetramers during HPLC size-exclusion chromatography, despite the observation

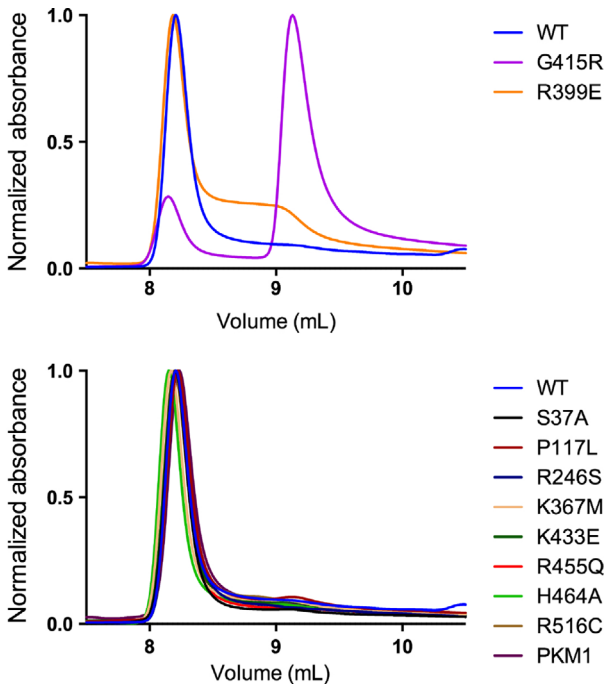

Fig. 9. HPLC size-exclusion chromatography of PKM2 and PKM2 mutants. PKM2 proteins were prepared using Prep 3, and then separated by HPLC size-exclusion chromatography in the absence of FBP to determine the effect of mutations on tetramer-monomer equilibrium. This separation method accommodates a high concentration of enzyme (0.5 mg·mL^{-1}) relative to the kinetic assays. An elution volume of ~ 8.25 mL is consistent with tetramers while an elution volume of ~ 9.25 mL is consistent with monomer. Only the G415R and R399E mutants showed significant amounts of protein eluting at a volume consistent with the enzyme being a dimer or monomer.

that maximal enzyme activity (V_{max}) from the same protein preparations could be increased by FBP, consistent with formation of active tetramers in a tetramer-dimer or tetramer-monomer equilibrium. These seemingly contradictory observations may be explained by the enzyme concentrations used in the respective assays. HPLC size-exclusion chromatography evaluates relatively concentrated samples (0.5 mg·mL^{-1}) that are a better approximation of cellular conditions than is the kinetic assay, which requires significant dilution of this highly active enzyme (to approximately 1 μg·mL^{-1} or 17 nM) to allow determination of initial rates. The *in vivo* concentration of pyruvate kinase has been reported as 172 μM or 10 mg·mL^{-1} [56], a value well above the reported K_D of 1 μM for tetramer-monomer and tetramer-dimer equilibria [18,39]. The HPLC size-exclusion results were thus obtained from samples at concentrations above the K_D for tetramer dissociation, while the kinetic assays can only be conducted with samples at concentrations below the K_D which favors tetramer dissociation. The kinetic assays employed by us and others for determining AC_{50} values for FBP activation of PKM2 are thus limited in that they measure the enzyme in an artificially dilute state, absent of the molecular crowding present in the cytosol. Our size-exclusion results differ from a recent report [18] in that we observe almost exclusively the tetramer form of PKM2 in the absence of FBP; this may be due to a number of factors in the current study, including a 5-fold greater concentration of protein, high flow rates allowed by HPLC that limit time-dependent dissociation of PKM2 tetramers, and the presence of Mg^{2+} available during separation to bind the active site and stabilize the protein. These data suggest that the majority of PKM2 in cells may exist in a tetrameric state rather than as mixture of inactive monomers/dimers and active tetramers.

The mutations that have been used to study non-canonical PKM2 functions were found to alter some aspect of PKM2 function as a glycolytic enzyme. The effect exhibited by these disparate mutations on enzyme kinetics suggests that generation of PKM2 mutations that abolish or alter specific protein functions is challenging. Therefore, interpretation of data relying on PKM2 mutants to study aspects of cell biology linked to cell proliferation also requires consideration of the metabolic consequences of those mutants.

The determination of kinetic parameters in this study was restricted to the analysis of PKM2 homomultimers. The cancer mutations reported are all heterozygous, suggesting that the mutated form of the enzyme is coexpressed with wild-type enzyme in the affected cancer cells. A similar situation has been found in individuals with Bloom syndrome, where heterozygous mis-sense mutations occur in PKM2 [53]. Like the mutations studied here, the single amino acid substitutions found in Bloom syndrome patients alter enzyme kinetics [54], despite the mutant subunits being capable of heterotetramerization with wild-type PKM2 [55]. PKM2 has been observed to form heterotetramers with PKM1 and PKL [20,61], and heterotetramerization is likely to occur between wild-type PKM2 and PKM2 mutants, as even chicken PKM1 and bovine PKL can form functional heterotetramers [62]. The kinetic parameters of heterotetramers containing wild-type and cancer mutant subunits remain to be determined, but they are likely to be intermediate between the kinetics of homotetramers of the two isoforms [63,64]. Because PKM2 and PKM1 differ by only one exon, they share significant sequence identity and four of the five cancer mutations studied here (P117L, R246S, R455Q, and R516C) would also occur in the M1 isoform if expressed in the cancer cell.

The presence of PKM2 mutations in human cancers demonstrates that some tumor cells tolerate, and perhaps select for, reduced PKM2 activity. PKM2 is not required for growth of many cancers [11,29,65–70], and loss-of-function mutations may be advantageous for cancer cells since decreased pyruvate kinase activity promotes a proliferative metabolic program [11,20,28,29]. Retention of one wild-type copy of PKM2 may provide metabolic flexibility by allowing upregulation of PKM2 activity to promote cancer cell survival under nutrient stress conditions [29]. Mutations in PKM2 are therefore not oncogenic, but may play a part in creating a metabolic state in the cancer cell that is permissive for proliferation. Regardless, this analysis demonstrates that the kinetic properties of PKM2 are sensitive to amino acid substitution and informs our understanding of how PKM2 impacts cancer biology.

Acknowledgements

The authors thank Katherine R. Mattaini and Katherine 'TK' Allsop for technical assistance. VML and AJH were supported by the MIT Undergraduate Research Opportunities Program. AMH was supported by an HHMI graduate student fellowship and was a Vertex Scholar. ZL and WJI were supported in part by T32GM007287. WJI also acknowledges support from the Sara and Frank McKnight Fund for Biochemical Research, and NIH DP5OD021365. MVH acknowledges support from NIH R01CA168653, P30CA1405141, the Burroughs Wellcome Fund, the Ludwig Center at MIT, SU2C, the Lustgarten Foundation, the MIT Center for Precision Cancer Medicine, and a Faculty Scholars Award from HHMI.

Conflict of interest

MGVH is a consultant and scientific advisory board member of Agios Pharmaceuticals, Aeglea Biotherapeutics, and Auron Therapeutics.

Author contributions

VML, AJH, AMH, ZL, and WJI performed the experiments and all authors contributed to writing the manuscript.

References

1 Mazurek S (2011) Pyruvate kinase type M2: a key regulator of the metabolic budget system in tumor cells. *Int J Biochem Cell Biol* **43**, 969–980.

2 Dayton TL, Jacks T and Vander Heiden MG (2016) PKM2, cancer metabolism, and the road ahead. *EMBO Rep* **17**, 1721–1730.

3 Harris RA and Fenton AW (2019) A critical review of the role of M2PYK in the Warburg effect. *Biochim Biophys Acta Rev Cancer* **1871**, 225–239.

4 Imamura K and Tanaka T (1972) Multimolecular forms of pyruvate kinase from rat and other mammalian tissues. I. Electrophoretic studies. *J Biochem* **71**, 1043–1051.

5 David CJ, Chen M, Assanah M, Canoll P and Manley JL (2010) HnRNP proteins controlled by c-Myc deregulate pyruvate kinase mRNA splicing in cancer. *Nature* **463**, 364–368.

6 Clower CV, Chatterjee D, Wang Z, Cantley LC, Vander Heiden MG and Krainer AR (2010) The alternative splicing repressors hnRNP A1/A2 and PTB influence pyruvate kinase isoform expression and cell metabolism. *Proc Natl Acad Sci USA* **107**, 1894–1899.

7 Morgan HP, O'Reilly FJ, Wear MA, O'Neill JR, Fothergill-Gilmore LA, Hupp T and Walkinshaw MD (2013) M2 pyruvate kinase provides a mechanism for nutrient sensing and regulation of cell proliferation. *Proc Natl Acad Sci USA* **110**, 5881–5886.

8 Taylor CB and Bailey E (1967) Activation of liver pyruvate kinase by fructose 1,6-diphosphate. *Biochem J* **102**, 32C–33C.

9 Koler RD and Vanbellinghen P (1968) The mechanism of precursor modulation of human pyruvate kinase I by fructose diphosphate. *Adv Enzyme Regul* **6**, 127–142.

10 Kahn A and Marie J (1982) Pyruvate kinases from human erythrocytes and liver. *Methods Enzymol* **90**, 131–140.

11 Dayton TL, Gocheva V, Miller KM, Israelsen WJ, Bhutkar A, Clish CB, Davidson SM, Luengo A, Bronson RT, Jacks T *et al.* (2016) Germline loss of PKM2 promotes metabolic distress and hepatocellular carcinoma. *Genes Dev* **30**, 1020–1033.

12 Chaneton B and Gottlieb E (2012) Rocking cell metabolism: revised functions of the key glycolytic regulator PKM2 in cancer. *Trends Biochem Sci* **37**, 309–316.

13 Gui DY, Lewis CA and Vander Heiden MG (2013) Allosteric regulation of PKM2 allows cellular adaptation to different physiological states. *Sci Signal* **6**, pe7.

14 Imamura K, Taniuchi K and Tanaka T (1972) Multimolecular forms of pyruvate kinase. II. Purification of M 2 -type pyruvate kinase from Yoshida ascites hepatoma 130 cells and comparative studies on the enzymological and immunological properties of the three types of pyruvate kinases, L, M 1, and M 2. *J Biochem* **72**, 1001–1015.

15 Dombrauckas JD, Santarsiero BD and Mesecar AD (2005) Structural basis for tumor pyruvate kinase M2 allosteric regulation and catalysis. *Biochemistry* **44**, 9417–9429.

16 Ashizawa K, McPhie P, Lin KH and Cheng SY (1991) An *in vitro* novel mechanism of regulating the activity of pyruvate kinase M2 by thyroid hormone and fructose 1, 6-bisphosphate. *Biochemistry* **30**, 7105–7111.
17 Chaneton B, Hillmann P, Zheng L, Martin AC, Maddocks OD, Chokkathukalam A, Coyle JE, Jankevics A, Holding FP, Vousden KH *et al.* (2012) Serine is a natural ligand and allosteric activator of pyruvate kinase M2. *Nature* **491**, 458–462.
18 Yuan M, McNae IW, Chen Y, Blackburn EA, Wear MA, Michels PAM, Fothergill-Gilmore LA, Hupp T and Walkinshaw MD (2018) An allostatic mechanism for M2 pyruvate kinase as an amino-acid sensor. *Biochem J* **475**, 1821–1837.
19 Macpherson JA, Theisen A, Masino L, Fets L, Driscoll PC, Encheva V, Snijders AP, Martin SR, Kleinjung J, Barran PE *et al.* (2019) Functional cross-talk between allosteric effects of activating and inhibiting ligands underlies PKM2 regulation. *ELife* **8**, e45068.
20 Anastasiou D, Yu Y, Israelsen WJ, Jiang JK, Boxer MB, Hong BS, Tempel W, Dimov S, Shen M, Jha A *et al.* (2012) Pyruvate kinase M2 activators promote tetramer formation and suppress tumorigenesis. *Nat Chem Biol* **8**, 839–847.
21 Ashizawa K, Willingham MC, Liang CM and Cheng SY (1991) *In vivo* regulation of monomer-tetramer conversion of pyruvate kinase subtype M2 by glucose is mediated via fructose 1,6-bisphosphate. *J Biol Chem* **266**, 16842–16846.
22 Merrins MJ, Van Dyke AR, Mapp AK, Rizzo MA and Satin LS (2013) Direct measurements of oscillatory glycolysis in pancreatic islet beta-cells using novel fluorescence resonance energy transfer (FRET) biosensors for pyruvate kinase M2 activity. *J Biol Chem* **288**, 33312–33122.
23 Christofk HR, Vander Heiden MG, Wu N, Asara JM and Cantley LC (2008) Pyruvate kinase M2 is a phosphotyrosine-binding protein. *Nature* **452**, 181–186.
24 Lv L, Li D, Zhao D, Lin R, Chu Y, Zhang H, Zha Z, Liu Y, Li Z, Xu Y *et al.* (2011) Acetylation targets the M2 isoform of pyruvate kinase for degradation through chaperone-mediated autophagy and promotes tumor growth. *Mol Cell* **42**, 719–730.
25 Anastasiou D, Poulogiannis G, Asara JM, Boxer MB, Jiang JK, Shen M, Bellinger G, Sasaki AT, Locasale JW, Auld DS *et al.* (2011) Inhibition of pyruvate kinase M2 by reactive oxygen species contributes to cellular antioxidant responses. *Science* **334**, 1278–1283.
26 Eigenbrodt E, Reinacher M, Scheefers-Borchel U, Scheefers H and Friis R (1992) Double role for pyruvate kinase type M2 in the expansion of phosphometabolite pools found in tumor cells. *Crit Rev Oncog* **3**, 91–115.
27 Christofk HR, Vander Heiden MG, Harris MH, Ramanathan A, Gerszten RE, Wei R, Fleming MD, Schreiber SL and Cantley LC (2008) The M2 splice isoform of pyruvate kinase is important for cancer metabolism and tumour growth. *Nature* **452**, 230–233.
28 Lunt SY, Muralidhar V, Hosios AM, Israelsen WJ, Gui DY, Newhouse L, Ogrodzinski M, Hecht V, Xu K, Acevedo PN *et al.* (2015) Pyruvate kinase isoform expression alters nucleotide synthesis to impact cell proliferation. *Mol Cell* **57**, 95–107.
29 Israelsen WJ, Dayton TL, Davidson SM, Fiske BP, Hosios AM, Bellinger G, Li J, Yu Y, Sasaki M, Horner JW *et al.* (2013) PKM2 isoform-specific deletion reveals a differential requirement for pyruvate kinase in tumor cells. *Cell* **155**, 397–409.
30 Stammers DK and Muirhead H (1977) Three-dimensional structure of cat muscle pyruvate kinase at 3–1 A resolution. *J Mol Biol* **112**, 309–316.
31 Muirhead H, Clayden DA, Barford D, Lorimer CG, Fothergill-Gilmore LA, Schiltz E and Schmitt W (1986) The structure of cat muscle pyruvate kinase. *EMBO J* **5**, 475–481.
32 Allali-Hassani A, Wasney GA, Chau I, Hong BS, Senisterra G, Loppnau P, Shi Z, Moult J, Edwards AM, Arrowsmith CH *et al.* (2009) A survey of proteins encoded by non-synonymous single nucleotide polymorphisms reveals a significant fraction with altered stability and activity. *Biochem J* **424**, 15–26.
33 Lu Z and Hunter T (2018) Metabolic kinases moonlighting as protein kinases. *Trends Biochem Sci* **43**, 301–310.
34 Amin S, Yang P and Li Z (2019) Pyruvate kinase M2: a multifarious enzyme in non-canonical localization to promote cancer progression. *Biochim Biophys Acta Rev Cancer* **1871**, 331–341.
35 Gao X, Wang H, Yang JJ, Liu X and Liu ZR (2012) Pyruvate kinase M2 regulates gene transcription by acting as a protein kinase. *Mol Cell* **45**, 598–609.
36 Yang W, Zheng Y, Xia Y, Ji H, Chen X, Guo F, Lyssiotis CA, Aldape K, Cantley LC and Lu Z (2012) ERK1/2-dependent phosphorylation and nuclear translocation of PKM2 promotes the Warburg effect. *Nat cell Biol* **14**, 1295–1304.
37 Hosios AM, Fiske BP, Gui DY and Vander Heiden MG (2015) Lack of Evidence for PKM2 protein kinase activity. *Mol Cell* **59**, 850–857.
38 Hitosugi T, Kang S, Vander Heiden MG, Chung TW, Elf S, Lythgoe K, Dong S, Lonial S, Wang X, Chen GZ *et al.* (2009) Tyrosine phosphorylation inhibits PKM2 to promote the Warburg effect and tumor growth. *Sci Signal* **2**, ra73.
39 Gavriilidou AFM, Holding FP, Mayer D, Coyle JE, Veprintsev DB and Zenobi R (2018) Native Mass spectrometry gives insight into the allosteric binding mechanism of M2 pyruvate kinase to fructose-1,6-bisphosphate. *Biochemistry* **57**, 1685–1689.

40 Blair JB and Walker RG (1984) Rat liver pyruvate kinase: influence of ligands on activity and fructose 1,6-bisphosphate binding. *Archiv Biochem Biophys* **232**, 202–213.

41 El-Maghrabi MR, Claus TH, McGrane MM and Pilkis SJ (1982) Influence of phosphorylation on the interaction of effectors with rat liver pyruvate kinase. *J Biol Chem* **257**, 233–240.

42 Cheng X, Friesen RH and Lee JC (1996) Effects of conserved residues on the regulation of rabbit muscle pyruvate kinase. *J Biol Chem* **271**, 6313–6321.

43 Le Mellay V, Houben R, Troppmair J, Hagemann C, Mazurek S, Frey U, Beigel J, Weber C, Benz R, Eigenbrodt E *et al*. (2002) Regulation of glycolysis by Raf protein serine/threonine kinases. *Adv Enzyme Regul* **42**, 317–332.

44 Luo W, Hu H, Chang R, Zhong J, Knabel M, O'Meally R, Cole RN, Pandey A and Semenza GL (2011) Pyruvate kinase M2 is a PHD3-stimulated coactivator for hypoxia-inducible factor 1. *Cell* **145**, 732–744.

45 Yang P, Li Z, Fu R, Wu H and Li Z (2014) Pyruvate kinase M2 facilitates colon cancer cell migration via the modulation of STAT3 signalling. *Cell Signal* **26**, 1853–1862.

46 Jiang Y, Wang Y, Wang T, Hawke DH, Zheng Y, Li X, Zhou Q, Majumder S, Bi E, Liu DX *et al*. (2014) PKM2 phosphorylates MLC2 and regulates cytokinesis of tumour cells. *Nat Commun* **5**, 5566.

47 Yang W, Xia Y, Ji H, Zheng Y, Liang J, Huang W, Gao X, Aldape K and Lu Z (2011) Nuclear PKM2 regulates beta-catenin transactivation upon EGFR activation. *Nature* **480**, 118–122.

48 Yang W, Xia Y, Hawke D, Li X, Liang J, Xing D, Aldape K, Hunter T, Alfred Yung WK and Lu Z (2012) PKM2 phosphorylates histone H3 and promotes gene transcription and tumorigenesis. *Cell* **150**, 685–696.

49 Bollenbach TJ, Mesecar AD and Nowak T (1999) Role of lysine 240 in the mechanism of yeast pyruvate kinase catalysis. *Biochemistry* **38**, 9137–9145.

50 Sakai H (2005) Mutagenesis of the active site lysine 221 of the pyruvate kinase from *Bacillus stearothermophilus*. *J Biochem* **137**, 141–145.

51 Wang P, Sun C, Zhu T and Xu Y (2015) Structural insight into mechanisms for dynamic regulation of PKM2. *Protein Cell* **6**, 275–287.

52 Williams R, Holyoak T, McDonald G, Gui C and Fenton AW (2006) Differentiating a ligand's chemical requirements for allosteric interactions from those for protein binding. Phenylalanine inhibition of pyruvate kinase. *Biochemsitry* **45**, 5421–5429.

53 Anitha M, Kaur G, Baquer NZ and Bamezai R (2004) Dominant negative effect of novel mutations in pyruvate kinase-M2. *DNA Cell Biol* **23**, 442–449.

54 Akhtar K, Gupta V, Koul A, Alam N, Bhat R and Bamezai RN (2009) Differential behavior of missense mutations in the intersubunit contact domain of the human pyruvate kinase M2 isozyme. *J Biol Chem* **284**, 11971–11981.

55 Gupta V, Kalaiarasan P, Faheem M, Singh N, Iqbal MA and Bamezai RN (2010) Dominant negative mutations affect oligomerization of human pyruvate kinase M2 isozyme and promote cellular growth and polyploidy. *J Biol Chem* **285**, 16864–16873.

56 Srivastava DK and Bernhard SA (1986) Metabolite transfer via enzyme-enzyme complexes. *Science* **234**, 1081–1086.

57 Murcott TH, Gutfreund H and Muirhead H (1992) The cooperative binding of fructose-1,6-bisphosphate to yeast pyruvate kinase. *EMBO J* **11**, 3811–3814.

58 Waygood EB, Mort JS and Sanwal BD (1976) The control of pyruvate kinase of *Escherichia coli*. Binding of substrate and allosteric effectors to the enzyme activated by fructose 1,6-bisphosphate. *Biochemistry* **15**, 277–282.

59 Xu YF, Zhao X, Glass DS, Absalan F, Perlman DH, Broach JR and Rabinowitz JD (2012) Regulation of yeast pyruvate kinase by ultrasensitive allostery independent of phosphorylation. *Mol Cell* **48**, 52–62.

60 Bennett BD, Kimball EH, Gao M, Osterhout R, Van Dien SJ and Rabinowitz JD (2009) Absolute metabolite concentrations and implied enzyme active site occupancy in *Escherichia coli*. *Nat Chem Biol* **5**, 593–599.

61 Cardenas JM and Dyson RD (1978) Mammalian pyruvate kinase hybrid isozymes: tissue distribution and physiological significance. *J Exp Zool* **204**, 361–367.

62 Cardenas JM, Blachly EG, Ceccotti PL and Dyson RD (1975) Properties of chicken skeletal muscle pyruvate kinase and a proposal for its evolutionary relationship to the other avian and mammalian isozymes. *Biochemistry* **14**, 2247–2252.

63 Cardenas JM and Dyson RD (1973) Bovine pyruvate kinases. II. Purification of the liver isozyme and its hybridization with skeletal muscle pyruvate kinase. *J Biol Chem* **248**, 6938–6944.

64 Hubbard DR and Cardenas JM (1975) Kinetic properties of pyruvate kinase hybrids formed with native type L and inactivated type M subunits. *J Biol Chem* **250**, 4931–4936.

65 Cortes-Cros M, Hemmerlin C, Ferretti S, Zhang J, Gounarides JS, Yin H, Muller A, Haberkorn A, Chene P, Sellers WR *et al*. (2013) M2 isoform of pyruvate kinase is dispensable for tumor maintenance and growth. *Proc Natl Acad Sci USA* **110**, 489–494.

66 Wang YH, Israelsen WJ, Lee D, Yu VW, Jeanson NT, Clish CB, Cantley LC, Vander Heiden MG and Scadden DT (2014) Cell-state-specific metabolic dependency in hematopoiesis and leukemogenesis. *Cell* **158**, 1309–1323.

67 Tech K, Tikunov AP, Farooq H, Morrissy AS, Meidinger J, Fish T, Green SC, Liu H, Li Y, Mungall AJ *et al.* (2017) Pyruvate kinase inhibits proliferation during postnatal cerebellar neurogenesis and suppresses medulloblastoma formation. *Cancer Res* **77**, 3217–3230.
68 Lau AN, Israelsen WJ, Roper J, Sinnamon MJ, Georgeon L, Dayton TL, Hillis AL, Yilmaz OH, Di Vizio D, Hung KE *et al.* (2017) PKM2 is not required for colon cancer initiated by APC loss. *Cancer Metab* **5**, 10.
69 Hillis AL, Lau AN, Devoe CX, Dayton TL, Danai LV, Di Vizio D and Vander Heiden MG (2018) PKM2 is not required for pancreatic ductal adenocarcinoma. *Cancer Metab* **6**, 17.
70 Dayton TL, Gocheva V, Miller KM, Bhutkar A, Lewis CA, Bronson RT, Vander Heiden MG and Jacks T (2018) Isoform-specific deletion of PKM2 constrains tumor initiation in a mouse model of soft tissue sarcoma. *Cancer Metab* **6**, 6.

Supporting information

Additional supporting information may be found online in the Supporting Information section at the end of the article.

Fig. S1. Structural location of cancer mutations.

Fig. S2. PKM2 prepared *via* a Two-Column Method (Prep 3) and Refolding (Prep 2) have comparable specific activities.

Fig. S3. Prep 3 allows reproducible kinetic results from independent batches of WT PKM2.

Fig. S4. Structural location of cancer mutations addressed in this study.

Fig. S5. The P117L mutation affects the "Hinge" allowing active site closure.

Fig. S6. The R246S mutation putatively disrupts structural contacts near the active site.

Fig. S7. The G415R mutation putatively disrupts tight packing at the Dimer-Dimer interface.

Fig. S8. The R455Q mutation putatively disrupts structural contacts near the FBP binding site.

Fig. S9. The R516C mutation is located on the FBP binding loop.

Fig. S10. S37 is solvent exposed.

Fig. S11. Residues K270 and K367 lie in the active site.

Fig. S12. K367 is near the ADP binding site but does not contact bound substrate.

Fig. S13. PKM2 mutants with reduced activity are effectively prepared *via* Prep 3.

Fig. S14. The R399E mutation disrupts favorable ionic contacts at the Dimer-Dimer interface.

Fig. S15. The K433E mutation disrupts the FBP-K433 interaction.

Fig. S16. H464 is located in the binding pocket of serine, alanine, and phenylalanine.

Table S1. Missense cancer mutations of PKM2 examined in this study.